General Relativistic Magnetohydrodynamic Simulations of Black Hole Accretion Disks: Results and Observational Implications

Julian H. KROLIK and Shigenobu HIROSE

Department of Physics and Astronomy, Johns Hopkins University, USA

A selection of results from the general relativistic MHD accretion simulations described in the previous talk are presented. We find that the magnetic field strength increases sharply with decreasing radius and is also enhanced near rapidly-spinning black holes. The greater magnetic field strength associated with rapid black hole rotation leads to a large outward electromagnetic angular momentum flux that substantially reduces both the mean accretion rate and the net accreted angular momentum per unit rest-mass. This electromagnetic stress strongly violates the traditional guess that the accretion stress vanishes at and inside the marginally stable orbit. Possible observational consequences include a constraint on the maximum spin of black holes, enhancement to the radiative efficiency, and concentration of fluorescent Fe Kα to the innermost part of the accretion disk.

§1. Introduction

In the preceding talk, John Hawley presented an overview of studies of MHD turbulence-driven accretion onto black holes. After outlining the principal physical mechanisms, he summarized how to simulate numerically such a system. At the close of his talk, he described the main structures that are seen. In this talk, I will report in greater detail some of the properties of the accretion flows observed in these simulations and indicate some of their implications for observations.

Ultimately, it is the magnetic field that controls how matter accretes, so the first topic in this review will be the distribution of field intensity, the topology of field-lines, and the way both depend on black hole spin (§II). Once this basis has been established, it will be possible to see how the magnetic field controls the accretion rate (§III). Accreting matter releases energy via dissipation of fluid motions and magnetic field; the heated gas can then generate photons. Although these simulations do not treat the thermodynamics of accretion explicitly, they do offer strong hints about how radiation may occur; some of these are discussed in §IV. We conclude this review with a list of some of the more interesting implications of our results (§V).

§2. Magnetic Field Structure

The most striking feature of the magnetic field is its extremely strong concentration toward the center of the system, especially when the black hole spins rapidly. We can characterize the strength of the field by the scalar $B^\mu B_\mu/(4\pi) \equiv ||b||^2$, the invariant squared-magnitude of the magnetic field four-vector, whose value is twice the magnetic field energy density measured in the fluid frame. As shown in Fig-

ure 1 (and discussed more thoroughly in[6]), $||b||^2$ rises steeply inward; averaged over spherical shells labelled by Boyer-Lindquist radius r, the scaling is roughly $\propto r^{-3}$ all the way from the inner radial boundary to the outer, a dynamic range of roughly two orders of magnitude in radius and six in magnetic energy density. Although the field intensity is more or less spherically distributed just outside the event horizon, it becomes flattened at those radii where the main disk body is found. Near the main disk body, the field is strongest near the disk surface, at the base of the corona.

It is also useful to characterize the field strength by its ratio to other relevant energy densities such as the gas's pressure and inertia. The "plasma β" is the ratio of gas to magnetic pressure. Inside the main disk body, we find it generally rather large, ~ 10–100. However, rising vertically away from the midplane, the gas density falls faster than the field strength, so that in the disk corona, $\beta \sim 1$, with excursions of factors of several both up and down. The ratio $||b||^2/(\rho h)$, where h is the specific enthalpy, indicates the relative importance of the gas's inertia to its (magnetically-driven) dynamics. When this ratio is $\gg 1$, the system is said to be "force-free", and there is a very large literature searching for "force-free" solutions to plasma dynamics near black holes. We find that this criterion is satisfied only in the outflow funnel, where the density is very low. Throughout the main disk body, the corona, and the inner disk, plasma inertia remains important, although the ratio of magnetic field strength to inertia rises to ~ 0.1 in the outer layers of the inflow through the plunging region.

The radial trend of magnetic intensity is especially sharp when the black hole spin parameter $a/M \geq 0.9$. Although the azimuthally-averaged $||b||^2$ does not change greatly with a/M at $r \simeq 25M$, at $r = 5M$, it grows by a full factor of ten as a/M increases from 0 to 0.998. This sensitivity of the field strength in the inner disk to black hole spin is likely a by-product of the way in which black hole spin also controls the accretion rate, as will be explained more fully in the next section.

In most regions, the field-line shapes are controlled by orbital shear (Fig. 2). In the main disk body, the strong turbulence creates loops and whorls, but the shear still makes the dominant field component toroidal. Contrary to intuition built from the Solar corona, the field in the disk corona does not have buoyant loops whose foot-points are twisted by turbulent motions in the disk. Rather, the field in the corona is combed extremely smooth by the shear. Because the dominant motion in the disk is regular circular orbits, there is little opportunity for loop-twisting. Because the fluid trajectories in the plunging region are dominated by ballistic infall rather than turbulence, the fieldlines there are drawn into a pattern as smooth as the one in the corona. The one region where the field is notably different is the outflow funnel. There, the field is essentially radial, as it is drawn out by the outward flow of matter, but close to the black hole it is twisted around by frame-dragging, as viewed in the Boyer-Lindquist coordinate frame.

§3. Magnetic Regulation of Accretion

Given the central role played by turbulence in driving accretion, it should not be surprising that the instantaneous accretion rate (i.e., the mass flux through the
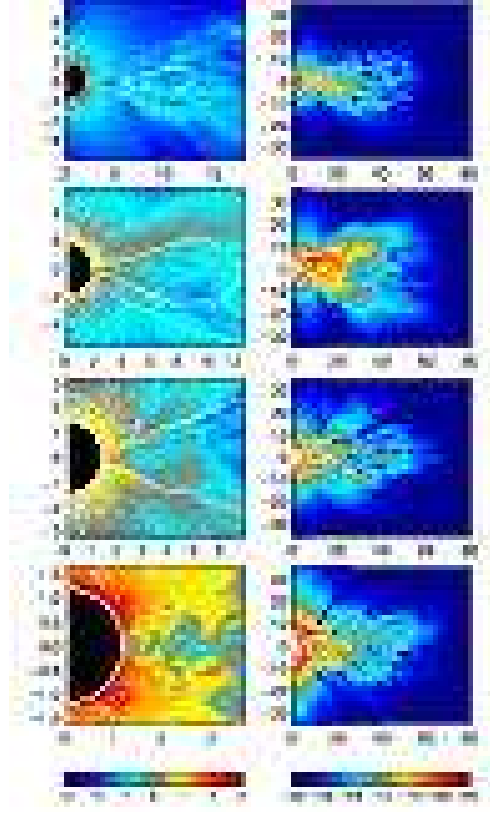
Fig. 1. Azimuthal-average of $(1/2)||b||^2$, the magnetic pressure in the fluid frame, normalized to the maximum initial gas pressure in the relevant simulation. The left column shows the region inside $r = 3r_{ms}$, plotted on a logarithmic scale that emphasizes the increasing dominance of magnetic pressure with black hole spin in the inner disk. The right column shows the main disk body with a different color scale (see color bars). The white dashed contours in the right column show where the gas pressure is 0.1, 1., and 10 times the initial maximum pressure.

inner boundary of the simulation) should vary. What is perhaps more surprising is two other facts (both illustrated in Fig. 3): that the variations occur over a wide range of timescales, from the dynamical time at the innermost stable circular orbit to much longer timescales; and that the mean accretion rate decreases sharply as the black hole spin increases.

The latter is a particularly noteworthy finding. Although we chose initial conditions for the four simulations that are very nearly identical, and the black hole spin makes little difference to the potential at radii $\gg 10M$, the amount of matter permitted to move inward through small radii diminishes by a factor of 4 as a/M rises from 0 to 0.998. Because the mean accretion rate just inside the initial pressure maximum (at $25M$ in all four cases) varies hardly at all with a/M, the diminution in accretion at rapid spin must—and does—result in a "pile-up" of matter at small radii. In all four simulations, an "inner torus" is created in the region just outside r_{ms}, but its mass grows with a/M. In fact, although its mass reaches an equilibrium
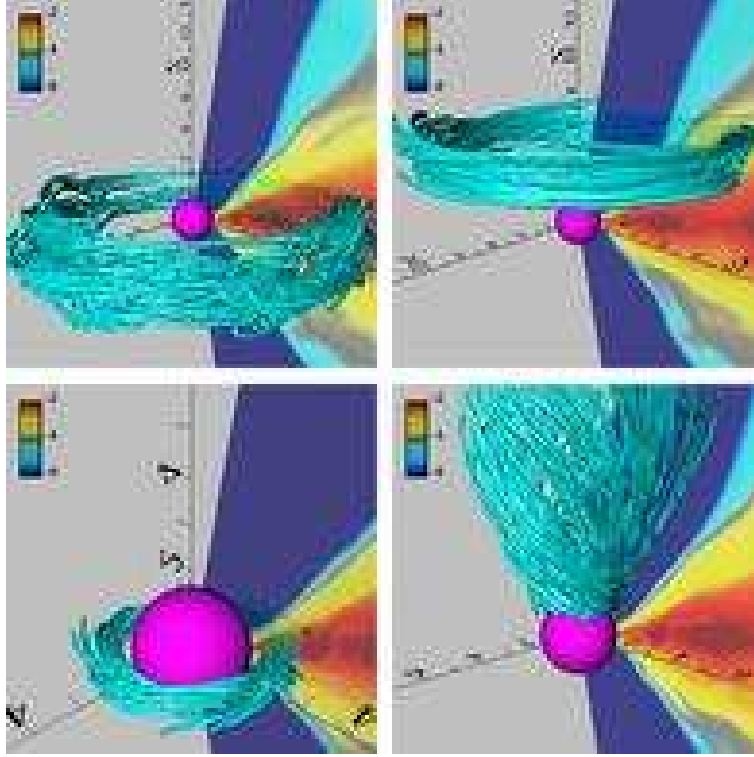
Fig. 2.   Sample field-lines (as seen in the coordinate frame) from a late-time snapshot of the simu-
       lation with $a/M = 0.9$. Upper left panel is the main disk body, upper right is the corona, lower
       left is the plunging region, lower right is the axial funnel. Background colors are contours of
       $\log(\rho)$, the proper rest-mass density, calibrated by the color-bar.

in the three simulations with $a/M \leq 0.9$, it grows steadily throughout the $8100M$ of
the simulation when $a/M = 0.998$. That the magnetic field in the inner disk grows
with a/M is a reflection of the general proportionality of the magnetic field intensity
to the local pressure in the main body of the disk, and the growth of the inner torus
with a/M.

   How this retardation of accretion is accomplished is most easily seen by studying
the time-average of the shell-integrated angular momentum flux. To be more precise,
the radial flux of axial angular momentum is

$$T^r_\phi = \rho h u^r u_\phi + ||b||^2 u^r u_\phi - b^r b_\phi, \tag{3.1}$$

where u^μ is the four-velocity. It is convenient to study the three pieces separately,
evaluating all quantities in the coordinate frame. The first we call the angular
momentum flux associated with matter, the second the angular momentum flux
of advected magnetic field, the third the angular momentum flux of the ordinary
accretion torque.

   When the magnetic torque rises outward, its net effect is to remove angular
momentum from matter, permitting the matter to move inward. A steady state
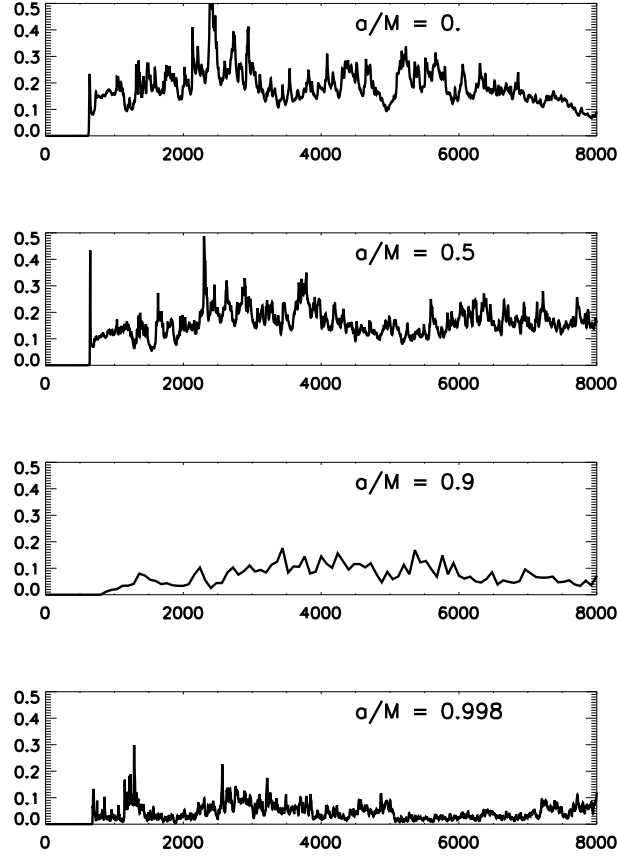can be achieved if those losses are balanced by gains associated with matter moving

Fig. 3. The accretion rate, in units of fraction of the initial mass per simulation duration, for each of the four simulations. The apparent absence of high-frequency variability in the $a/M = 0.9$ simulation is an artifact of the lower data-recording rate employed for that simulation.

inward. That is the case everywhere outside r_{ms} for the $a/M = 0$ and $a/M = 0.5$ simulations, but it is *not* what happens in the two simulations with more rapid spin (Fig. 4). In both the $a/M = 0.9$ and $a/M = 0.998$ cases, the time-average magnetic torque *adds* to the matter's angular momentum over a substantial radial range starting near r_{ms} and extending outward. Moreover, the magnitude of the outward magnetic angular momentum flux rises sharply with increasing black hole spin, becoming comparable to the inward angular momentum flux associated with accreting matter when $a/M \geq 0.9$. As a result, accretion is retarded and the mass in these rings grows. This is the origin of both the partial suppression of accretion with faster black hole spin and also the inner torus.

The question immediately arises: what is the source of this outward angular momentum flux carried by the magnetic field? The obvious answer is: the central black hole. What we are witnessing here is a process analogous to the classical Blandford-Znajek effect,[2] in which magnetic fields threading the event horizon of a
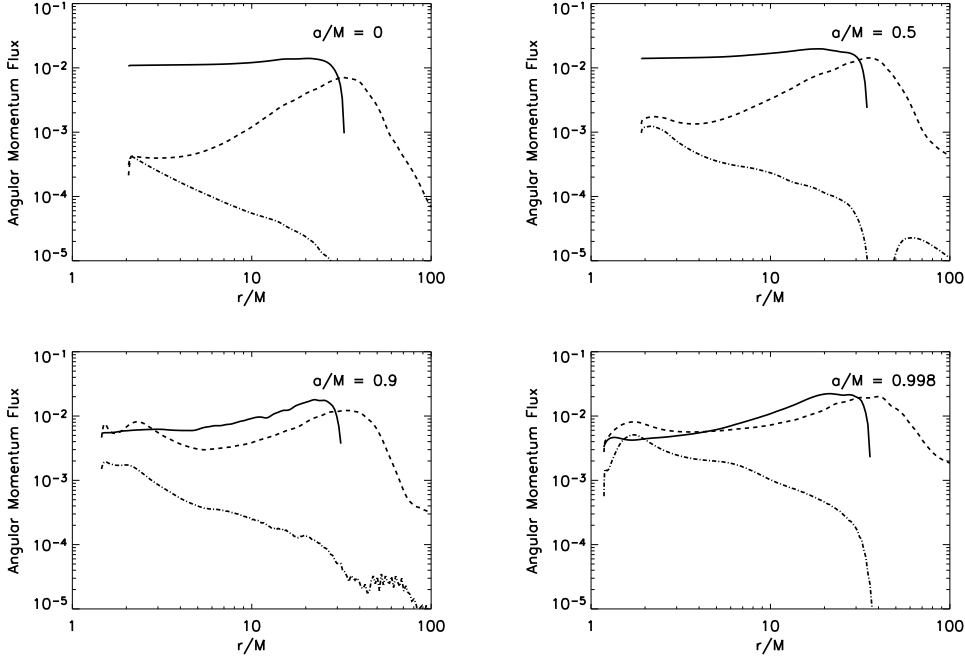
Fig. 4. Absolute values of the shell-integrated and time-averaged (for times later than $2000M$) angular momentum fluxes in each of the four simulations. All angular momentum fluxes are normalized to the initial pressure maximum of the relevant simulation to ease comparison of different simulations. The solid curve is the matter flux, the dashed curve is the magnetic torque, the dot-dash curve is the part due to advected magnetic field. The actual signs are such that the matter flux and advected magnetic field carry (prograde) angular momentum inward, the magnetic torque outward.

rotating black hole are able to carry angular momentum and energy out to infinity. In our case, the field lines don't precisely thread the event horizon, but that's unnecessary: passage through the ergosphere is the essential requirement. Likewise, the field lines of greatest importance here do not wind out in a helix around the rotation axis, stretching to infinity; rather, they curve around in the accreting matter, mostly staying within $\simeq 45°$ of the equatorial plane.

In this context, it is important to point out that the strength of the stresses throughout the marginally stable region demonstrates that the heuristic "zero-stress" boundary condition guessed thirty years ago[8),9)] does not in fact apply. As was feared at the time,[9)] magnetic fields void the plausibility arguments in favor of this boundary condition.

§4.   Dissipation

In real disks, orbital shear energy is transformed into magnetic field energy, and magnetic field energy is dissipated into heat by a variety of resistive processes acting most effectively where there are sharp field gradients. Our simulations contain

no explicit resistivity; instead, purely numerical effects mimic genuine resistivity by destroying field energy where the field gradients are large. Because most microphysical models of genuine dissipation predict that it rises very rapidly with increasing current density, we can identify candidate dissipation regions in our simulation data by computing the scalar current density-squared $J^\mu J_\mu$, where $J^\mu = (1/4\pi)\nabla_\mu F^{\mu\nu}$ for Maxwell field tensor $F^{\mu\nu}$ and covariant derivative ∇_μ.

We find that the regions of strong current are highly intermittent; that is, they tend to be organized into sheet-like structures in which the current density can change by several orders of magnitude when travelling a very short distance along the local normal to the sheet. In addition, both the probability per unit volume of finding a strong current region and the strength of the current found there increase dramatically toward small radii. Finally, given the substantally stronger magnetic field of the simulations with more rapidly spinning black holes, it is no surprise that the characteristic level of current density is also highest when a/M is relatively large.

Because many of the most intense current regions are located within the marginally stable orbit, we speculate that the plunging region may be the site of substantial dissipation. This energy release would be over and above the conventional energy release associated with stress in the disk body, as envisioned in the original papers.[8),9)] If the local temperature can be raised high enough to make inverse Compton scattering the primary radiation mechanism, the cooling time becomes much shorter than the freefall time if there is even a modest intensity of soft photons.[6)] Some of the Compton-scattered photons will go onto capture orbits, but it is possible that the fraction escaping could still represent an interesting addition to the radiative output of the system.

§5. Implications

Our new understanding of accretion onto black holes suggests changes in the conventional thinking about both the dynamics of accreting black holes and their radiative properties.

The most obvious consequence of the large diminution in the net angular momentum per unit mass accreted is that black holes may spin up less rapidly than thought, and it may not be possible for accretion to make them spin faster than some maximum a/M, perhaps $\simeq 0.9$.[3),5)] A likely corollary of the continued stress that reduces the accreted angular momentum is additional energy dissipation and a consequent increase in the fraction of the accreted rest-mass that is radiated; a quantitative determination of this demands a more complete treatment of accretion thermodynamics and radiation diffusion. Another consequence of the strong outward electromagnetic angular momentum flux, particularly when a/M is comparatively large, is the creation of a massive "inner torus" just outside the marginally stable orbit, a structure in the disk surface density distribution never envisioned in the standard treatments because they generally assumed a fixed proportionality between stress and integrated pressure.[11)] Lastly, it is clear from these simulations that there are consistently large amplitude fluctuations in virtually every dynamical quantity and across a wide range of timescales.

Any increase in the radiative efficiency is likely to be concentrated in the innermost part of the accretion flow. The extra photons produced should therefore be largely at higher energies. Because of the strong relativistic beaming, boosting, and photon trajectory-bending deep in the black hole potential, these photons will be especially noticeable when our view of the disk is more-or-less edge-on; in addition, a significant fraction of them will return to the disk at larger radii, to be reprocessed there.[1]

Additional "coronal" activity in the inner disk may concentrate the excitation of fluorescent Fe Kα emission in that region. There already appears to be observational evidence for this,[4,12] possibly including Kα emission from the plunging region.[7,10]

Finally, the ubiquitous dynamical fluctuations are a likely source for the "rednoise" fluctuations that are ubiquitous in black-hole light-curves. To predict the power spectrum of luminosity fluctuations resulting from the dynamical fluctuations also awaits a better treatment of accretion thermodynamics and photon diffusion, both of which can filter the dynamical fluctuation power spectrum, but the general scheme seems to be very promising.

Acknowledgements

References

1) E. Agol and J. H. Krolik, Astrophys. J. **528**, 161 (2000)
2) R. D. Blandford and R. Znajek, Mon. Not. Roy. Ast. Soc. **179**, 433 (1977)
3) J. P. De Villiers, J. F. Hawley, and J. H. Krolik, Astrophys. J., **599** (2003), 1238.
4) A. C. Fabian et al., Mon. Not. Roy. Ast. Soc. **335**, L1 (2002)
5) C. F. Gammie, S. L. Shapiro, and J. C. McKinney, Astrophys. J., in press (2004).
6) S. Hirose, J. H. Krolik, J.-P. De Villiers, and J. F. Hawley, Astrophys. J., in press (2004).
7) J. H. Krolik, and J. F. Hawley, Astrophys. J., **573** (2002), 754.
8) I. D. Novikov, and K. S. Thorne, in *Black Holes—Les Astres Occlus*, ed. C. De Witt (Gordon and Breach, New York, 1972), 346.
9) D. N. Page and K. S. Thorne, Astrophys. J. **191**, 499 (1974)
10) C. S. Reynolds and M. C. Begelman, Astrophys. J. **488**, 109 (1997)
11) N. I. Shakura, and R. A. Sunyaev, Astron. Astrophys., **24** (1973), 337.
12) J. Wilms et al., Mon. Not. Roy. Ast. Soc. **328**, L27 (2001)